Journal of Water Science and Engineering

Research Article

Adsorption of Dyes from Water on to Bamboo-Based Activated Carbon - Error Analysis Method for Accurate Isotherm Parameter Determination

AkankshaKalra[1], Hadi P[1], Hui CW[1], Mackey H[2], Ansari TA[2], Saleem J and McKay G[2*]

[1]Department of Chemical and Biomolecular Engineering, Hong Kong University of Science and Technology, Clear Water Bay Road, Hong Kong

[2]Division of Sustainability, College of Science and Engineering, Hamad Bin Khalifa University, Education City, Qatar Foundation, Doha, Qatar

Volume 1 Issue 1 - 2019
Received Date: 25 Jan 2019
Accepted Date: 06 Feb 2019
Published Date: 11 Feb 2019

2. Keywords

Error analysis; Dye adsorption; Bamboo; Activated carbon; Reactive Black

1. Abstract

The adsorption of Reactive Black 5 dye from aqueous solution been studied using four types of adsorbents, namely BACX6 (Bamboo Activated Carbon), BACX2, Filtrasorb F400 and bone char.It is important to determine the most accurate capacity parameters from isotherm studies in order determine the size of an adsorption water treatment process. The experimental results obtained showed that BAXC2 has the highest BET surface area of 2123 m2/g followed by BAXC6 which has 1400 m2/g , F400 793 m2/g and bone char 107 m2/g. Equilibrium isotherms were determined by seven methods using Langmuir, Freundlich, Langmuir-Freundlich (L-F), Redlich-Peterson (R-P), Toth, Temkin and Dubinin-Radushkevich (D-R) isotherms models. Five error analysis methods were used to obtain the best fit model: the sum of errors squared, hybrid error function, Marquardt's percent standard deviation, the average relative error and sum of the absolute error. The results showed that the R-P model gave the best results for BACX6 and BACX2, whereas the L-F gave the best results for F400 and bone char using the hybrid error function.

3. Introduction

Water pollution is becoming a serious concern due to the increasing contamination by industrial pollutants in fresh water bodies [1]. Many processes like the pulp and paper, plastics, leather treatment and printing industries use a wide range of dyes and discharge them into the aquatic ecosystems [2]. In the textile industries, large quantities of dyestuffs rereleased into water bodies with residual dye liquors through washing, rinsing and dyeing process operations and it is essential that removal techniques must be adopted [3]. Dyes are stable to heat and are both resistant to light and are non-biodegradable. Based on these characteristic properties they pose significant threats to the environment and consequently need to be treated in an effective manner [4]. Nevertheless, dye containing effluents are difficult to treat as they are highly stable, frequently contain toxic metal ions and complexes with high quantities of total dissolved solids [5,6].

Treatment techniques, including coagulation-flocculation, membrane separation, reverse osmosis and solvent extraction, have been used to process these problematic effluents [7,8]. However, several of these treatment technologies generate their own problems including, the associated high cost, large volumes of sludge formation and the subsequent disposal problems. Alternatively, adsorption, as a flexible, simple and inexpensive approach, can be used for dye process effluent treatment so reducing the concerns over high operating and capital costs, efficiency and the need for secondary treatment [9]. A wide range of adsorbent materials have been developed and tested over the years and applied for efficient dye removal. Activated carbon is the most widely-used adsorbent because of its low cost, exceptionally-high porosity, tuneablepore size and high adsorptive capacities [10]. Many types of agricultural waste by-products, such as husk [11,12], fruit and vegetable shells [13,14], fruit stones [15], oil-palm shell [16,17], bagasse [18-23], pine cone [24] and bamboo [25-27], have shown potential as precursors for activated carbon production.

Several natural materials [28-32] have been tested for their dye removal capabilities, including peat, sawdust, lignite and wastes

***Corresponding Author (s):** Gordon McKay, Division of Sustainability, College of Science and Engineering, Hamad Bin Khalifa University, Education City, Qatar Foundation, Doha, Qatar, Tel: +97444541408, E-mail: gmckay@hbku.edu.qa*

Citation: AkankshaKalra, Hadi P, Hui CW, Mackey H, Ansari TA, Saleem J and McKay G, Adsorption of Dyes from Water on to Bamboo-Based Activated Carbon - Error Analysis Method for Accurate Isotherm Parameter Determination. Journal of Water Science and Engineering. 2019; 1(1): 1-11.

such as tyre chars [33-37].

Among these precursors, bamboo holds great potential for activated carbon preparation as a carbonaceous material possessing 44 wt% carbon content. Other benefits include its application as a major scaffolding material throughout Asia followed by its disposal as a waste material after use [38]. In addition, it can be applied as a sustainable resource as one of the world's most rapidly growing plants at a rate in excess of one meter per year.

In this project, the sorption of a dye, Reactive Black 5, from aqueous solution onto bamboo-derived activated carbon has been studied and the dye adsorption capacities have been compared with other activated carbons. In order to design adsorption process plants to treat coloured effluents, it is essential to have very accurate data to predict the treatment system capacity. The equilibrium isotherms have been analyzed using seven isotherm models and five error analysis methods which have been used to correlate the data and obtain the best fit equilibrium model. These error functions have been normalized across the range of all the error functions for a more accurate basis of comparison and selection of the most suitable error function which has further been used to find the most accurate isotherm constants.

4. Materials and Methods

4.1. Adsorbate

In order to investigate the efficiency of the activated carbon produced for dye adsorption, Reactive Black 5 (Chemical formula = $C_{26}H_{21}N_5Na_4O_{19}S_6$, MW = 991.8 g/mol, and λ_{max} = 599 nm), widely used in the textile industries, has been selected as adsorbent. The dye was supplied by International Laboratory (USA), and the structure is presented in Figure 1. A one thousand ppm (mg/L) stock solution was prepared by dissolving the required amount of the dye in deionized water and the solutions for the experiments were prepared by diluting the stock solution.

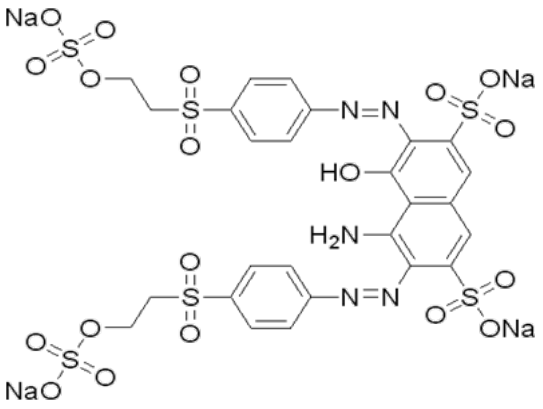

Figure 1: Molecular structure of the Reactive Black 5.

4.2 Adsorbent preparation

Bamboo activation to activated carbons was carried out using phosphoric acid as the activating agent and has been described in detail [38]. Briefly, crushed bamboo was soaked using 85% phosphoric acid to a predetermined impregnation ratio. This resulting material was then pre-treated in the muffle furnace at 150˚C for 120 minutes and then carbonized at 600˚C for 240 minutes in an inert gas flow of nitrogen. After carbonization, this activated material was cooled and washed with hot deionized water until the wash water pH was 5.5. Two bamboo impregnation ratios were used resulting in two carbon products, namely, 2:1 (BACX2) and 6:1 (BACX6). In addition, two other adsorbents were tested, bone char (supplied by Brimac) and F400 (supplied by Calgon) were used in the adsorption studies. The particle size of bone char and F400 used for the studies ranged between 500-710 μm and powdered activated carbon (< 180 μm) was used for bamboo activated carbon.

4.3 Chemical and physical characterization of the adsorbents

The surface acidic and basic functional groups were determined by the Boehm titration method [30]. For the measurement of surface acidity, 0.2 g of adsorbents were contacted with 50 ml of 0.05N standard NaOH and shaken for 2 days. The mixture was filtered and then back-titrated with 0.05N standard HCl. For the measurement of surface basicity, 0.2g of adsorbents were contacted with 50 ml of 0.05N standard HCl and shaken for 2 days. The mixture was filtered and then back-titrated with 0.05 N standard NaOH. Titrations were employed to determine the point of zero charge of the adsorbents. Different masses of adsorbent materials within the concentration range 5–100 g/L were put into contact with a 0.01M of KCl solution and shaken for 24 hours until equilibrium pH was reached. The pH_{pzc} is the pH at which a plateau is achieved when plotting equilibrium pH versus adsorbent mass.

The textural properties of the adsorbents were obtained by determining the nitrogen adsorption/desorption isotherm at -196ºC using a QuantachromeAutosorb 1. The specific surface area was calculated using the BET equation (S_{BET}) and the total pore volume (V_p) was evaluated based on the amount of nitrogen adsorbed at a relative pressure of P/P^o =0.97 and the average pore diameter was determined using the relationship: $D_p = 4V_p / S_{BET}$. The pore size distribution of the adsorbents was estimated using the Barrett, Joyner and Halenda model [39].

4.4 Adsorption Studies

Equilibrium adsorption studies for Reactive Black dye 5 were conducted by contacting 50 ml of dye solution of different initial concentrations with 0.05 g of adsorbent in glass bottles. The bot-

tles were shaken until equilibrium is reached. Upon equilibration, solutions were filtered through 0.22µm syringe filter, and analysed by UV-visible spectrophotometer (Ultrospec 4300 Pro) at its maximum absorbance (λ_{max}= 599 nm)to determine the residual equilibrium liquid-phase dye concentration. The equilibrium adsorption capacity, q_e (mg/g), at different dye concentrations was determined by a mass balance on the dye:

$$m = (q_o - q_e) = V(C_o - C_e) \quad (1)$$

Since: q_o = O, then,

$$q_e = \frac{V(C_o - C_e)}{m}\frac{V(C_o - C_e)}{m} \quad (2)$$

where C_0 (mg/L) is the initial concentration, C_e (mg/L) is the equilibrium concentration in the liquid phase, V is the volume of liquid phase (L), and m is the mass of the adsorbent (g).

5. Theory

5.1. Equilibrium studies

An adsorption process reaches equilibrium when the amount of dye being adsorbed onto the adsorbent is equal to the amount being desorbed at constant temperature and pH conditions. The performance of an adsorption process can be analyzed by plotting the adsorbed dye concentration (q_e) against the equilibrium dye concentration in the liquid phase (Ce), q_e being the dependent variable. Equilibrium isotherm models are frequently used to predict or analyze the performance of adsorption processes and determine parameters like adsorption capacity. In this study, equilibrium experiments have been conducted to find the most suitable equilibrium isotherm by evaluating and comparing errors of each isotherm and subsequently finding the optimized parameters.

5.2. Error functions

Error functions are used to evaluate how well the isotherm fits the experimental result. The choice of error function will affect obtained isotherm parameters. Thus we need to compare different error functions to find the function giving the least error. Error functions based on absolute deviation from original values bias the fit towards higher concentrations data. This is the case with SSE. This bias can be avoided by taking fractional deviations. In every isotherm case, each error function is minimized across all the concentration range studied. All the error analysis methods used in this project have been listed below:

SSE/ERRSQ (Sum ofSquared Errors)

$$\sum (q_{e,exp} - q_{e,cal})^2 \quad (3)$$

The parameters $q_{e,exp}$ and $q_{e,cal}$ are the experimental and calculated capacities of the adsorbed material, respectively.

Eq (3) represents the most commonly-used error function, but it has a major drawback. As the magnitude of the errors and thus the squares of the errors increase there is a biasing of the fit towards the data obtained at the high end of the concentration range.

b) HYBRID (Hybrid Fractional Error Function)

$$\frac{100}{n-p}\sum \frac{(q_{e,exp} - q_{e,cal})^2}{q_{e,exp}} \quad (4)$$

This error function in Eq (4) was developed in an attempt to improve the fit of the sum of the squares of the errors at low concentrations by dividing it by the measured value. The parameters n and p indicate the number of data points and number of parameters, respectively [40].

c) MPSD (Derivative of Marquardt's Percent Standard Deviation)

$$100 \times \sqrt{\frac{1}{n-p}\sum \frac{(q_{e,exp} - q_{e,cal})}{q_{e,exp}}} \quad (5)$$

This error function, Eq (5), was used previously by a number of researchersin the field. It is similar in some respects to a geometric mean error distribution modified according to the number of degrees of freedom of the system [41].

d) ARE (Average Relative Error)

$$\frac{100}{n}\sum \left|\frac{(q_{e,exp} - q_{e,cal})}{q_{e,exp}}\right| \quad (6)$$

This error function shown in Eq (6)attempts to minimize the fractional error distribution across the entire concentration range [42].

e) EABS (Sumof Absolute Errors)

$$\sum |q_{e,exp} - q_{e,cal}| \quad (7)$$

This approach, represented by Eq. (7) is similar to the sum of the squares of the errors. Isotherm parameters determined using this error function would provide a better fit as the magnitude of the error increases, biasing the fit towards the high concentration data [43].

An error analysis is performed to compare the errors of all the equilibrium isotherm models and find out which one most closely fits the experimental data – this correlation will then yield the most accurate isotherm constants. In this project, Solver add-in was used in Microsoft Excel 2013 to carry out the optimizations. In the end, all the errors were normalized to accurately compare the errors on a common basis.

5. Results and Discussion

5.1. Characterization of adsorbents

5.1.1. Physical characterization of adsorbents: The adsorption of organic compounds is controlled by both physical and chemical interactions between the adsorbates and the adsorbents. The physical characteristics of the adsorbent control the admiltanceof molecules to the micro – and mesoporesinside the carbon. The accessible adsorbent surface is especially important for the adsorption of large molecules such as synthetic organic chemicals and naturally occurring organic materials. The physical characteristics of the adsorbents are summarized in Table 1[38], indicating that the adsorbents have significant differences in surface area, pore volume and average pore diameter. Adsorbent pores can be divided into micropores (pore size < 2 nm) and mesopores (pore size ranged between 2-50 nm). The commercial activated carbon F400 has a typical high surface area; it has a larger volume of micropores than mesopores and the smallest average pore diameter, indicating that the carbon has a higher micro porosity.

Both bamboo activated carbons have a much higher surface area and pore volume compared with other adsorbents and BACX2 resulting in the highest surface area and micro pore volume, whereas, BACX6 has the highest mesopore volume. The bamboo activated carbon produced has a much higher surface area than other activated carbons produced using other lignocellulosic materials and phosphoric acid activation [44]. Bone char has a relatively low surface area due to its lack of micro porosity which normally contributes most surface area.

5.1.2. Chemical characterization of adsorbents: The adsorbent chemical properties affect the attractive or repulsive interactions and the acidity/bascity and $pH_{PZC}$are important chemical characteristics of adsorbents as they determine the net charge of the adsorbent in the solution. The chemical characteristics of the adsorbents are shown in Table 2. The results showed that F400 contains both acidic and basic characteristics. Typically, the acid functional groups in activated carbons include carboxylic, lactonic, and phenolic species, and the basic functional groups include ketones, pyrones, as well as chromene species. F400 has more basic properties and has a relatively low density of surface functional groups. The combined effect of all functional groups determines the pH_{pzc} which is slightly alkaline for F400 whereas bamboo activated carbon has more acidic properties and has a relatively high density of surface functional groupings such as phosphate-containing carbonaceous structures like acid phosphates and polyphosphates which are present on the surface of synthetic phosphoric acid-activated carbons [44]. This result shows that the bamboo carbon $pH_{pzc}$is the lowest for all the adsorbents in this study. Bone char also showed more basic properties, and the basic and acidic sites are formed by the protonation and deprotonation of the hydroxyapatite surface hydroxyl groups [45].

Table 1: Textural properties of the four adsorbents.

Adsorbent	S_{BET}(m²/g)	V_{micro}(cm³/g)	V_{meso}(cm³/g)	D_p (nm)
F400	793	0.141	0.123	2.44
Bone Char	107	0	0.255	9.43
BACX2	2123	0.494	0.943	2.79
BACX6	1400	0.209	2.008	5.32

5.2. Equilibrium isotherms for reactive dye adsorption on activated carbon

The equilibrium liquid phase concentration (C_e) was measured and their adsorption capacity (q_e) was calculated for each adsorbent. The results which are expressed as plots of solid phase dye concentration against liquid phase dye concentration are shown in Figure 2.

The highest dye adsorption capacities occurs on both bamboo activated carbons, because both bamboo activated carbons have a much higher surface area and pore volume than the other adsorbents. In Table 1, BACX2 has a higher surface area than that of BACX6, however the adsorption capacity of BACX6 is higher. And this is due to the fact that BACX6 has a much higher mesopore volume than BACX2 – 2.008 cm³/g versus 0.943 cm³/g - and the mesopore volume is important for adsorbing large molecules [46,47].

Table 2: Acidity, basicity and point of zero charge (pH_{pzc}) of the five adsorbents.

Adsorbent	Total acidic groups (mmol/g)	Total basic groups (mmol/g)	pH_{pzc}
F400	0.396	0.420	7.33
Bone char	0.13	3.067	9.83
BACX2	2.52	0.045	1.84
BACX6	2.50	0.150	1.93

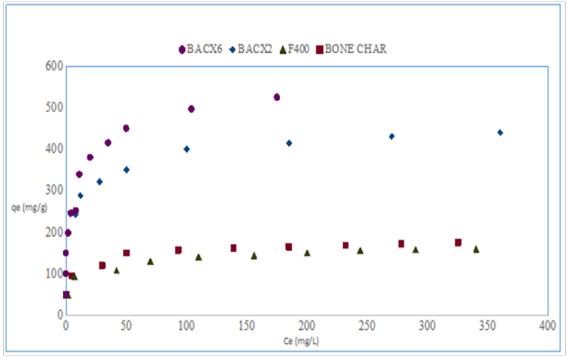

Figure 2: Experimental adsorption capacities of the four adsorbents.

In addition to pore size distribution and surface area, the adsorbent surface chemistry is critical in controlling the adsorption mechanism. The adsorbents have a net positive charge and vice versa when on the surface when the equilibrium pH of the solution is higher than the pH_{pzc} of the adsorbents the equilibrium solution pH is lower than the $pH_{pzc.}$ Both F400 and bone char have an overall positive charge as the final equilibrium pH ranging from 6-6.8 for F400 and 7.5-9 for bone char which is lower than the pH_{pzc} of the adsorbents. Consequently electrostatic attraction, which favours the adsorption process, appeared positive on the surface and favoured the adsorption of the negative Reactive Black 5 dye molecules.

BACX2 and BACX6 both have a net negative charge on the surface as the final equilibrium ranged from 3.4-3.5 which is higher than the pH_{pzc} of the adsorbents. Reactive dyes and the surface of the bamboo activated carbon are also negatively charged and still the reactive dyes are adsorbed to a significant extent. This suggested the effect of Van der Waals attraction and π-π forces seem to be dominant and control the adsorption as the bamboo activated carbons have a much higher surface area than the other adsorbents [48,49]. also suggested that π-π dispersion interactions dominate the adsorption process when most of the surface is unavailable for adsorption of co-ionic species. In addition, under a highly acidic environment, the Reactive Black dye is not fully ionized and the surface of activated bamboo is not fully negatively charged which can reduce the repulsion of the dye molecules at the carbon surface and enhance the adsorption process.

5.3. Isotherm models

The equilibrium isotherms are of importance in the practical design and operation of adsorption systems. Seven isotherm models, namely, Langmuir, Freundlich, Sips, Tempkin, Toth, D-R and Redlich-Peterson were employed to describe the adsorption of Reactive Black dye5. A minimizing procedure was applied to solve each isotherm equation by minimizing the sum of error square (SSE) between the theoretical data for q_e calculated from the equations and the experimental data points.

5.3.1 The Langmuir isotherm: Langmuir suggested an equilibrium theory to describe the monolayer coverage of an adsorb ate a homogenous adsorbent surface [50]. The Langmuir isotherm assumes that sorption takes place at specific homogenous sites within the adsorbent. Once an adsorb ate molecule occupies a site, no further adsorption can take place at that site. Therefore, an equilibrium value can be achieved and the saturated monolayer curve can be expressed by Eq (8) as: where q_e is the solid phase

$$q_e = \frac{K_L C_e}{1 + a_L C_e} \qquad (8)$$

concentration of adsorbed species at equilibrium (mg/g), *Ce* is the equilibrium concentration of the adsorb ate in the solution at equilibrium (mg/L), a_L is the Langmuir isotherm constant (L/g) and K_L is Langmuir isotherm constant (L/g). Equation (8) obeys the Henry's Law at low concentrations and is applicable to homogenous sorption where the sorption of each sorbate molecule on the surface has equal sorption activation energy. The ratios K_L/a_L gives the theoretical monolayer saturation capacity, q_o (mg/g). The isotherm constants, a_L, K_L, q_o and minimum error functions are presented in **Table 3**. The monolayer capacities of F400, bone char, BACX2 and BACX6 are 148, 165, 406 and 489 mg/g respectively. The adsorption isotherm data of Reactive Black 5 onto various adsorbents were correlated with the Langmuir model as shown in **Figure 3**.

Table 3: Langmuir constants with error analysis for RB5 dye.

	K_L (L/g)	a_L (L/mg)	q_0 (mg/g)	Least Error Method	Least Normalized Error Value
BACX6	110.5	0.2256	489.9	EABS	3.805
BACX2	114.9	0.2823	407.0	ERRSQ	4.746
F400	35.76	0.2402	148.8	ERRSQ	3.337
Bone char	46.25	0.2799	165.2	ERRSQ	3.989

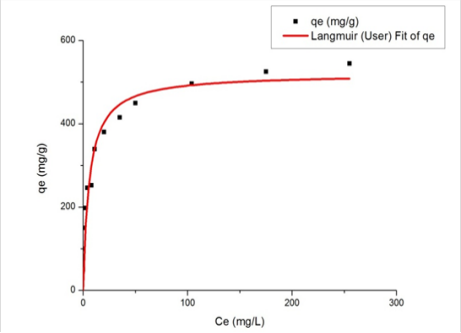

Figure 3: Langmuir isotherm fitting for Black Reactive Dye 5 onto Bamboo Activated carbon BACX6. Solid symbols represent experimental data.

The q_0 values show that BACX6 has the highest monolayer adsorption capacity and it also fits the best. Although, the high magnitudes of errors suggest that Langmuir isotherm is not a very good model for the sorption of Reactive Black dye 5 on the four activated carbons. Lastly, ERRSQ gives the best approximation to the parameter values for three of the adsorbents and EABS gives the best approximation for BACX6.

Table 4 demonstrates the difference in the isotherm constants that the choice of error analysis method can make. The differences in a_L range from 0.1749 to 0.2545, a difference of 45% and the monolayer capacity, q_m, varies from 475.5 to 519.4 mg dye/g adsorbent, a difference of 9.2%.

A similar table can be generated for each isotherm model and similar variations in the isotherm constants are observed. These

additional tables are not reproduced in the paper but are provided as Supplementary Materials.

5.3.2 Freundlich isotherm: In 1906, Freundlich suggested a model to describe the properties of heterogeneous systems [51]. This model has been widely applied in heterogeneous adsorption systems especially for organic compounds and high interactive species on activated carbon. The studies from Freundlich showed that the ratio of the amount of solute adsorbed onto a given mass of adsorbent to the concentration of the solute in the solution was not a constant at different solution concentrations. Freundlich proposed this multi-site adsorption isotherm for heterogeneous surface and expressed it in Eq (9) as:

$$q_e = K_F C_e^{b_F} \quad (9)$$

where q_e is the solid phase concentration of adsorbed species at equilibrium (mg/g), *Ce* is the equilibrium concentration of the adsorbate in the solution at equilibrium (mg/L), K_F is the Freundlich constant (L/g) and b_F is the heterogeneity factor. The Freundlich constant is an empirical constant depending on several environment factors. The factor b_F ranges between 0 and 1. It indicates the degree of non-linearity between solution concentration and adsorption. If the value of is b_F equal to unity, the adsorption is linear, which means q_e value is proportional to C_e value; if the value is below unity, the adsorption process is chemical like the cases in this report; if the value is above unity, adsorption is more likely to be a physical process.

The equation predicts that the adsorbed dye concentration will increase as long as the dye concentration in the liquid increases. According to the error analysis done, this isotherm has very high magnitudes of error for all the error functions. This is also proved by the fact that the isotherm figures do not demonstrate good fittings. HYBRID error function gives the least error for two adsorbent materials and ARE gives the least error for bone char and BACX2.

5.3.3 Sips isotherm model : The Sips isotherm, Eq (10), is derived by combining the Langmuir and the Freundlich expressions [52]. It is used to predict the heterogeneous adsorption systems.

$$q_e = \frac{q_m . K_{lf} . C_e^{\frac{1}{n_{lf}}}}{1 + . K_{lf} . C_e^{\frac{1}{n_{lf}}}} \quad (10)$$

At low adsorb ate concentrations equation (10) reduces to Freundlich equation but does not obey Henry's law. The exponent n_{LF} accounts for the heterogeneity of the system and when n_{LF}=1, the equation approaches the Langmuir equation. The isotherm constants for the Sips model are shown in Table 6 for dyes and the fitting is plotted for ERRSQ in **Figure 7**.

The K_{LF} values vary quite a lot across the range of error functions, with BACX6 giving the least error using HYBRID error function. The fitting of the isotherm model is good and the error analysis gives good results.

5.3.4 Redlich-Peterson isotherm model: The Redlich-Peterson isotherm is a hybrid isotherm featuring both Langmuir and Freundlich isotherms shown in Eq (11) and does not follow monolayer adsorption[53].

$$q_e = \frac{K_R C_e}{1 + a_R C_e^{\beta}} \quad (11)$$

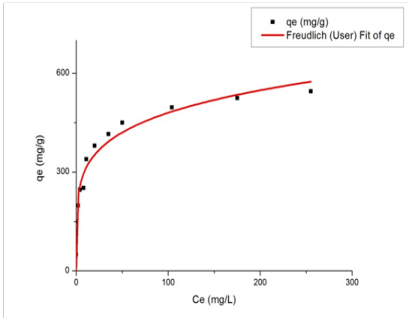

Figure 4: Freundlich isotherm fitting for Black Reactive Dye 5 onto Bamboo Activated carbon BACX6. Solid symbols represent experimental data.

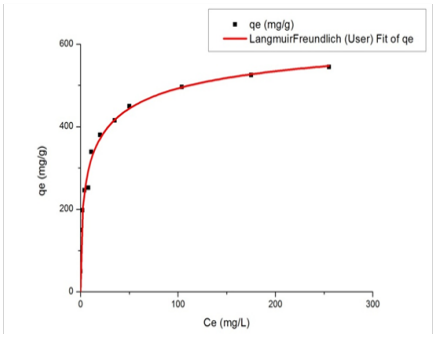

Figure 5: Sips isotherm fitting for Black Reactive Dye 5 onto Bamboo Activated carbon BACX6. Solid symbols represent experimental data. Again the constants - KLF values-vary quite substantially across the range of error functions, with BACX6 giving the least error using HYBRID error function. The fitting of the isotherm model is good and the error analysis gives good results.

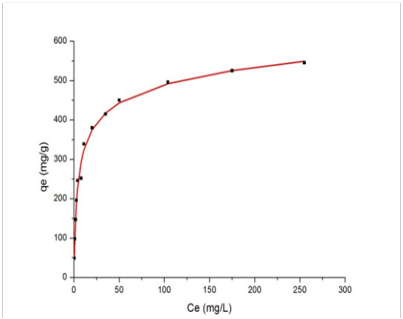

Figure 6: R-P isotherm fitting for Black Reactive Dye 5 onto Bamboo Activated carbon BACX6. Solid symbols represent experimental data.

It is an empirical equation with three parameters, K_R (L/g), a_R (L/mg) and β. The exponent β lies between 0 and 1. When β=1, the equation is equal to Langmuir equation; when β=0, it becomes Henry's law.

Dye adsorption onto BACX6 using the R-P model gives the following results as shown in **Table 7** and isotherm fitting is shown in **Figure 6**.

5.3.5 Temkin isotherm model: The Temkin isotherm represented by Eq (12) is the early model describing the adsorption of hydrogen onto platinum electrodes within the acidic solutions. This model is excellent in describing gas adsorption systems. An assumption is made that heat of adsorption (function of temperature) of all molecules in the layer would decrease linearly rather that logarithmically with surface coverage [54].

$$q_e = \alpha \ln K_t + \alpha \ln C_e \qquad (12)$$

Table 4: Error analysis for Langmuir isotherm for BACX6.

BAXC6	ERRSQ	HYBRID	MPSD	ARE	EABS
q_0(mg/g)	519.4	502.1	475.5	487.5	489.9
a_L(L/mg)	0.1749	0.2084	0.2545	0.2402	0.2256
SSE	**9242.0**	10540.0	16270.0	13550.0	12410.0
HYBRID	40.03	**34.82**	42.03	38.22	36.11
MPSD	0.2782	0.1755	**0.1372**	0.1405	0.1519
ARE	1.466	1.184	1.014	**1.007**	1.059
EABS	305.2	299.0	322.1	299.4	**294.8**
SUM of NE	4.468	3.842	4.185	3.864	**3.805**

Table 5: Freundlich constants with error analysis for RB5 dye.

	K_F (L/g)	1/n	Least Error Method	Least Normalized Error Value
BACX6	127.3	0.2916	HYBRID	3.084
BACX2	165.3	0.1760	ARE	4.437
F400	48.00	0.2250	HYBRID	2.981
Bone char	66.16	0.1751	ARE	3.659

Table 6: Sips constants with error analysis for RB5 dye.

	q_m (L/g)	K_{LF} (L/mg)	$1/n_{LF}$	Least Error Method	Least Normalized Error Value
BACX6	571.3	0.2180	0.7409	HYBRID	3.509
BACX2	448.8	0.3013	0.7173	ARE/EABS	3.339
F400	196.3	0.2196	0.5368	ERRSQ	4.684
Bone char	230.2	0.3775	0.3679	ERRSQ	4.688

Table 7: R-P constants with error analysis for RB5 dye.

	K_R (L/g)	a_R (L/mg)	β	Least Error Method	Least Normalized Error Value
BACX6	150.0	0.4767	0.8967	ERRSQ	4.375
BACX2	268.4	0.6420	0.9142	ARE/EABS	4.246
F400	83.03	0.6012	0.8796	ERRSQ	4.396
Bone char	81.13	4.755	0.8633	MPSD	4.416

The Temkin isotherm constants for Black Reactive Dye 5 adsorption onto BACX6 are listed in **Table 8**.

The least error value for BACX6 is again provided by ERRSQ and for BACX2 it is HYBRID. The error values provided are moderate in magnitude which are also shown by the isotherm fittings. EABS provides the best fit for the other two adsorbents.

5.3.6 Toth isotherm model: The Toth isotherm is derived from potential theory and is applicable to heterogeneous adsorption [55]. According to the theory there is a quasi-Gaussian energy distribution. The energy levels of most adsorption sites are lower than the peak or maximum adsorption energy. It obeys Henry's law at low concentration. The Toth isotherm equation (13) has the following form:

$$q_e = \frac{K_T C_e}{(\alpha_T + C_e{}^{\beta})^{\frac{1}{\beta}}} \qquad (13)$$

Table 8: Temkin constants with error analysis for RB5 dye.

	α	K_t	Least Error Method	Least Normalized Error Value
BACX6	81.09	4.215	ERRSQ	4.503
BACX2	59.57	6.981	HYBRID	2.765
F400	23.42	3.888	EABS	4.783
Bone char	18.81	33.85	EABS	4.812

Table 9: Toth constants with error analysis for RB5 dye.

	K_T (L/g)	β	α_T	Least Error Method	Least Normalized Error Value
BACX6	607.3	0.5781	1.790	HYBRID	4.344
BACX2	474.2	0.5261	1.150	HYBRID	3.585
F400	206.1	0.4077	0.5817	ARE/EABS	4.675
Bone char	271.2	0.2247	0.3816	ARE/EABS	4.720

The Toth isotherm constants for Black Reactive Dye 5 adsorption onto BACX6 are listed in **Table 9**.

The Toth model for the first adsorbents gives a good estimate of the isotherm parameters using HYBRID error functions.

Note1: For the Toth isotherm error analysis with F400 and bone char, ARE and EABS both provide the least error values. However, while minimising one of the two errors it would give the minimum value for corresponding both errors i.e. EABS and ARE. Thus, to optimize the result different initial parameter values are tried until both the error functions converge to the same values

5.3.7 D-R isotherm model: The Dubinin-Radushkecitch (D-R) equation was initially proposed as an empirical adaptation of the Polanyi adsorption potential theory [56]. Since then it has been the fundamental equation to quantitatively describe the gas adsorption and vapor adsorption by microporous adsorbents in the form of Eq (14). The mechanism for adsorption in micropores is that of pore-filling rather than layer-by-layer surface coverage.

$$\ln q_e = \ln q_D - B_D\left(RT\ln\left(1+\frac{1}{C_e}\right)\right)^2 \qquad (14)$$

The D-R isotherm constants for Black Reactive Dye 5 adsorption onto BACX6 are listed in **Table 10**.

The D-R model gave the highest error values for all the adsorbents. This is also observed in the isotherm models, wherein the isotherm curves do not fit the experimental results at all. The HYBRIB error analysis gave the least error for BACX6, BACX2 and F400; but in the case of bone char the ARE method provided the lowest error.

5.4. Error Analysis

5.4.1Best Error Function: In Table 11, the normalised errors having the least values for the corresponding isotherm models and adsorbents for dyes are summarised. A comparison of all the normalised errors obtained for each isotherm model was made and the least error was noted. This step was repeated for all the four adsorbents.

From **Table 11**, we observe that the HYBRID error gives the least errors in 9 out of 28 systems, EABS gives the best in 8, ERRSQ in 8 and ARE in 6. Therefore we compare the isotherms on the basis of the HYBRID error function.

5.4.2. Best fit model: From Table 11, the HYBRID model would be chosen as the best error function. Thus, we compared the error values of all the isotherms for each dye system using the HYBRID error values. The isotherm giving the least error value is listed in Table 12. This step was repeated for all the four dye systems. Among the four adsorption systems, the L-F and R-P both gave the best fits for two systems each.

Table 10: D-R constants with error analysis for RB5 dye.

	q_D	B_D	Least Error Method	Least Normalized Error Value
BACX6	420.9	1.011E-006	HYBRID	4.724
BACX2	333.6	3.036E-07	HYBRID	4.236
F400	158.4	1.037E-04	ARE/EABS	4.923
Bone char	168.9	5.37E-05	EABS	4.993

Table 11: Composite table for normalised errors having the least values for RB5 dye.

	BACX6	**BACX2**	**F400**	**Bone char**
Langmuir	3.8055 (EABS)	4.7460 (ERRSQ)	3.3372 (ERRSQ)	3.9895 (ERRSQ)
Freudlich	3.0837 (HYBRID)	4.4374 (ARE)	2.9806 (HYBRID)	3.6592 (ARE)
Sips	3.5088 (HYBRID)	3.3391 (ARE/EABS)	4.6842 (ERRSQ)	4.6883 (ERRSQ)
Redlich-Peterson	4.3746 (ERRSQ)	4.2457 (HYBRID)	4.3964 (ERRSQ)	4.4162 (MPSD)
Temkin	4.5033 (ERRSQ)	2.7652 (HYBRID)	4.7831 (EABS)	4.8117 (EABS)
Toth	4.3445 (HYBRID)	3.5846 (HYBRID)	4.6754 (ARE/EABS)	4.7200 (ARE/EABS)
D-R	4.7242 (HYBRID)	4.2356 (HYBRID)	4.9229 (ARE/EABS)	4.9931 (EABS)

Table 12: Best fit model for different adsorption isotherms for dyes based on HYBRID error function.

Activated Carbon	**Best Fit Model**	**HYBRID**
BACX6	R-P	10.19
BACX2	R-P	17.13
F400	L-F	2.533
Bone Char	L-F	1.613

6. Conclusions

The L-F and R-P isotherms provided the least error value overall for all the four adsorbents of the Reactive Black 5 dye systems and its isotherm curves also fit well to the experimental data. Individually, R-P gave the best values for BACX6 and BACX2, while the L-F model gave the best values for F400 and bone char. Thus, these isotherms will be the most suitable ones to determine adsorption parameters. HYBRID seemed to give the best result for most of the models followed by ERRSQ and EABS. The D-R model gave the worst fit isotherm and its values did not correlate well with the experimental values, giving high magnitudes of er-

ror. The effect of the choice of error analysis method selected to analyse data has been demonstrated to influence the magnitude of the isotherm parameters; in the Langmuir example, by 45% for a_L and by 9.2% for q_m. This is very significant in adsorption system design applications.

References

1. Belaid KD, Kacha S, Kameche M, Derriche Z. Adsorption kinetics of some textile dyes onto granular activated carbon. J Envir Chem Eng. 2013;1(3):496-503.

2. Hadi P, Sharma SK, McKay G. Removal of Dyes from Effluents Using Biowaste-Derived Adsorbents, in: S.K. Sharma (Ed.), Green Chem. Dye. Removal from Wastewater Res. Trends Appl., Scrivener Publishing LLC, 2015:139-201.

3. Robinson T, Mcmullan G, Marchant R, Nigam P. Remediation of dyes in textile effluent: a critical review on current treatment technologies with a proposed alternative. Bioresour Technol. 2001;77(3):247-55.

4. Lin L, Zhai SR, Xiao ZY, Song Y, Da An Q, Song XW. Dye adsorption of mesoporous activated carbons produced from NaOH-pretreated rice husks. Bioresour Technol. 2013;136:437-43.

5. Chan LS, Cheung WH, Allen SJ, McKay G. Error analysis of adsorption isotherm models for acid dyes onto bamboo derived activated carbon. Chinese J Chem Eng. 2012;20(3):535-42.

6. Tezcan U, Ates F, Erginel N, Ozcan O, Oduncu E. Adsorption of Disperse Orange 30 dye onto activated carbon derived from Holm Oak (Quercus Ilex) acorns : A 3k factorial design and analysis. J Envir Manage. 2015;155:89-96.

7. Yu L, Luo YM. The adsorption mechanism of anionic and cationic dyes by Jerusalem artichoke stalk-based mesoporous activated carbon. J Envir Chem Eng. 2014;2(1):220-9.

8. Mezohegyi G, van der Zee P, Font J, Fortuny A, Fabregat A. Towards advanced aqueous dye removal processes: A short review on the versatile role of activated carbon. J Environ Manage. 2012;102:148-64.

9. Hadi P, Yeung KY, Barford J, An KJ, McKay G. Significance of "effective" surface area of activated carbons on elucidating the adsorption mechanism of large dye molecules. J Environ Chem Eng. 2015;3(2):1029-37.

10. da Silva Lacerda V, López-Sotelo JB, Correa-Guimarães A, Hernández-Navarro S, Sánchez-Báscones M, Navas-Gracia LM, et al. Rhodamine B removal with activated carbons obtained from lignocellulosic waste. J Environ Manage. 2015;155:67-76.

11. Guo Y, Rockstraw DA. Activated carbons prepared from rice hull by one-step phosphoric acid activation. Micro Meso Mater. 2007;100(1-3):12-9.

12. Wu FC, Wu PH, Tseng RL, Juang RS. Preparation of novel activated carbons from H2SO4-Pretreated corncob hulls with KOH activation for quick adsorption of dye and 4-chlorophenol. J Environ Manage. 2011;92(3):708-13.

13. Aboua KN, Yobouet YA, Yao KB, Goné DL, Trokourey A. Investigation of dye adsorption onto activated carbon from the shells of Macoré fruit. J Environ Manage. 2015;156:10-4.

14. Nadeem M, Tan IB, Haq MRU, Shahid SA, Shah SS, McKay G. Sorption of lead from aqueous solution by chickpea leaves, stems and fruit peelings. Ads. Sci. Technol. 2006;24(3):269-82.

15. Ugurlu M, Gürses A, Açikyildiz M. Comparison of textile dyeing effluent adsorption on commercial activated carbon and activated carbon prepared from olive stone by ZnCl2 activation. Microporous Mesoporous Mater. 2008;111(1-3):228-35.

16. Tan IAW, Hameed BH, Ahmad AL. Equilibrium and kinetic studies on basic dye adsorption by oil palm fibre activated carbon. Chem Eng J. 2007;127(1-3):111-9.

17. Ahmad A, Loh M, Aziz J. Preparation and characterization of activated carbon from oil palm wood and its evaluation on Methylene blue adsorption. Dye Pigment. 2007;75(2):263-72.

18. Chen B, Hui CW, McKay G. Film-Pore Diffusion Modeling and Contact Time Optimisation for the Adsorption of Dyes on Pith. Chem Eng J. 2001;84(2):77-94.

19. Önal Y, Akmil-Başar Ç, Sarici-Özdemir C, Erdogan S. Textural development of sugar beet bagasse activated with ZnCl2. J Hazard Mater. 2007;142(1-2):138-43.

20. Valix M, Cheung WH, McKay G. Preparation of activated carbon using low temperature carbonisation and physical activation of high ash raw bagasse for acid dye adsorption. Chemosphere. 2004;56(5):493-501.

21. McKay G, Yee TF, Nassar MM, Magdy Y. Fixed Bed Adsorption of Dyes on Bagasse Pith. Ads Sci Technol. 1998;16(8):623-39.

22. McKay G, Geundi EM, Nassar MM. Adsorption Model for the Removal of Acid Dyes from Effluent by Bagasse Pith. Ads Sci Technol. 1997;15(10):737-52.

23. McKay G, Geundi EM, Nassar MM. Equilibrium Studies for the Adsorption of Dyes on Bagasse Pith. Ads Sci Technol. 1997;15(4):86-197.

24. Samarghandi M, Hadi M, McKay G. Breakthrough curve analysis for fixed bed adsorption of azo dyes using novel pine cone-derived active carbon. Ads Sci Technol. 2014;32(10):791-806.

25. Mui ELK, Cheung WH, Valix M, McKay G. Dye adsorption onto char from bamboo. J Hazard Mater. 2010;177(1-3):1001-5.

26. Wang L. Application of activated carbon derived from "waste" bamboo culms for the adsorption of azo disperse dye: Kinetic, equilibrium and thermodynamic studies. J Environ Manage. 2012;102 :79-87.

27. Chan LS, Cheung WH, McKay G. Adsorption of acid dyes by bamboo derived activated carbon. Desalination. 2008;218(1-3):304-12.

28. McKay G, Allen SJ, McConvey IF, Otterburn MS. Transport processes in the sorption of coloured ions by peat particles. J Coll Interf Sci. 1981;80(2):323-39.

29. cKay G, Allen SJ. Single resistance mass transfer models for the adsorption of dyes on peat. J Sepn Proc Technol. 1983;4(3):1-7.

30. McKay G, Allen SJ, McConvey IF, Walters HRJ. External transfer and homogenous solid phase diffusion during the adsorption of dyestuffs. Ind Chem Proc Des Dev. 1984;23:221-6.

31. McKay G, Allen SJ, McConvey IF. The adsorption of dyes from solution - equilibrium and column studies. Wat Air Soil Pollut. 1984;21(1-4):127-39.

32. Allen SJ, McKayG, KhaderKYH. Equilibrium adsorption isotherms for basic dyes onto lignite. J Chem Technol Biotechnol. 1989;45(4):291-302.

33. Chan OS, Cheung WH, McKay G. Single and multicomponent acid dye adsorption equilibrium studies on tyre demineralised activated carbon. Chem Eng J. 2012; 191:162-170.

34. Ho YS, McKay G. Application of Kinetic Models to the Sorption of Copper(II) on to Peat. Ads Sci Technol. 2002; 20(8):797-815.

35. Ho YS, McKay G, Wase DAJ, Forster CF. Study of the Sorption of DivalentMetal Ions on to Peat. Ads Sci Technol. 2000;18(7):639-50.

36. McKay G, Vong B, Porter JF. Isotherm Studies for the Sorption of Metal Ions onto Peat. Ads Sci Technol. 1998;16(1):51-66.

37. McKay G, Ho YS. Kinetic Model for Lead (II) Sorption onto Peat. Ads Sci Technol. 1998;16(4):243-55.

38. Ip AW, Barford JP, McKay G. Production and comparison of high surface area bamboo derived active carbons. Bioresour Technol. 2008;99(18):8909-16.

39. Al-Degs Y, Khraisheh MAM. Allen SJ, Ahmad MN. Effect of carbon surface chemistry on the removal of reactive dyes from textile effluent. Water Res. 2000;34(3):927-35.

40. Sing K. Reporting gas/solid data for physisorption system with special reference tothe determination of surface area and porosity, Pure Appl. Chem. 1985;57(4):603-19.

41. Porter JF, McKay G, Choy KH. The prediction of sorption from a binarymixture of acidic dyes using single- and mixed-isotherm variants of the ideal adsorbed solute theory. Chem Eng Sci. 1999;54(24):5863-85.

42. Marquardt DW. An algorithm for least-squares estimation of nonlinear parameters. J Soc Ind Appl Math. 1963;11(2):431-41.

43. Seidel A, Gelbin D. On applying the ideal adsorbed solution theory tomulticomponent adsorption equilibria of dissolved organic components on activated carbon. Chem Eng Sci. 1988;43(1):79-88.

44. Hameed BH, Tan IAW, Ahmad AL. Adsorption isotherm, kinetic modelingand mechanism of 2,4,6-trichlorophenol on coconut husk-based activated carbon. Chem Eng J. 2008;144(2):235-44.

45. Valix M, Cheung WH, McKay G. Roles of the textural and surface chemical properties of activated carbon in the adsorption of acid blue dye. Langmuir. 2006;22(10):4574-82.

46. Allen SJ, McKay G, Porter JF. Adsorption isotherm models for basic dye adsorption by peat in single and binary component systems. J Colloid Interface Sci. 2004;280(2):322-33.

47. Koumanova B, Peeva P, Allen S. Variation of intraparticle diffusion parameterduring adsorption ofp-chlorophenol onto activated carbon made from apricot stones. J Chem Technol Biotechnol. 2003;78(5):582-7.

48. Radovic LR, Silva IF, Ume JI, Menéndez JA, Leon CALY, Scaroni AW. An experimental and theoretical study of the adsorption of aromatics possessingelectron-withdrawing and electron-donating functional groups by chemically modified activated carbons. Carbon. 1997;35:1339-48.

49. Michailof C, Stavropoulos GG, Panayiotou C. Enhanced adsorption of phenolic compounds, commonly encountered in olive mill wastewaters, on olive husk derived activated carbons. Bioresour Technol. 2008;99:6400-8.

50. Langmuir I. The adsorption of gases on the plane surfaces of glass, mica and platinum. J Am Chem Soc. 1918;40(9):1361-403.

51. Freundlich HMF. Over the adsorption in solution. J Phys Chem A. 1906;57:385-471.

52. Sips R. On the Structure of a Catalyst Surface. J Chem Phys. 1948;16:490-5.

53. Redlich O, Peterson DL. A useful adsorption isotherm. J Phys Chem. 1959;63(6):1024.

54. Temkin MI, Pyzhev V. Kinetics of ammonia synthesis on promoted ironcatalyst, Acta Physicochim. URSS. 1940;12:327-56.

55. Toth J. State equations of the solid gas interface layer, Acta Chim. Acad Sci Hung. 1971;69:311-28.

56. Dubinin MM. The potential theory of adsorption of gases and vapors for adsorbents with energetically nonuniform surfaces. Chem Rev. 1960; 60(2):235-41.